AIAA JOURNAL
Vol. 50, No. 3, March 2012

Vibration Analysis of Composite Sandwich Plates by the Generalized Differential Quadrature Method

A. Arikoglu* and I. Ozkol†
Istanbul Technical University, 34469 Istanbul, Turkey

DOI: 10.2514/1.J051287

In this study, the vibration and damping analysis of a three-layered sandwich plate with composite face layers and a viscoelastic core is considered. The governing equations and related boundary conditions are derived in terms of sectional force and moment resultants by using the principle of virtual work for free vibrations of the plate. The eigenvalue problem defined by these equations is solved by using the generalized differential quadrature method to obtain the frequencies and loss factors. Results are compared with the ones that exist in the literature for three plate problems. Lastly, a parametric analysis is carried out for sandwich plates with carbon fiber reinforced plastic face layers and a frequency-dependent viscoelastic core. Viscoelastic behavior is modeled based on the five-parameter fractional Zener model. The master curves and material properties of four different viscoelastic polymers are obtained from the experimental data that exist in the literature. The effects of these polymeric damping materials on the vibration and damping characteristics of the sandwich plate are thoroughly studied. The eigenproblem is also solved by using the finite element method to verify the results of the generalized differential quadrature method.

Nomenclature

a, b	=	dimensions of the plate
$c_{ik}^{(p)}$, $d_{jm}^{(r)}$	=	weighting coefficients
E_1, E_2	=	Young's moduli
f	=	circular frequency
G_0	=	static moduli
G_{13}, G_{12}, G_{23}	=	shear modulus
G_∞	=	high-frequency moduli
h_i	=	thickness of ith layer
N_{xx}, N_{yy}	=	normal force components
N_{xy}, N_{xz}, N_{yz}	=	shear force components
$\mathbf{K}$, $\mathbf{M}$	=	stiffness and mass matrices
M_{xy}, M_{xz}, M_{yz}	=	moment components
$\bar{Q}_{mn}^{(i)}$	=	transformed stiffness coefficients for the ith layer
T	=	actual temperature
T_A	=	activation temperature
T_0	=	reference temperature
u, v, w	=	displacements in x, y, and z directions
u_0, v_0	=	displacements of the centroid of the core in x and y directions
α, β	=	fractional-order time derivatives
ε_{xx}, ε_{yy}	=	normal strain components
ε_{xy}, ε_{xz}, ε_{yz}	=	shear strain components
η	=	loss factor
θ	=	angle of lamination
ν	=	Poisson's ratio
ξ	=	error tolerance
ρ	=	density
σ_{xx}, σ_{yy}	=	normal stress components
σ_{xy}, σ_{xz}, σ_{yz}	=	shear stress components
τ	=	relaxation time
φ, γ	=	rotations of normals to midplane about the x and y axis
ω	=	complex eigenfrequency

Received 23 March 2011; revision received 4 August 2011; accepted for publication 4 August 2011.

*Research Assistant, Aeronautical Engineering Department.
†Professor, Aeronautical Engineering Department.

I. Introduction

VIBRATION induced stresses and displacements are major problems, which may cause unwanted noise and fatigue that may lead to the failure of a component or the structure itself. Therefore, damping and reduction of these vibrations are of great importance and damping layers that consist of viscoelastic materials are commonly used to achieve this goal. These materials can either be adapted during the design stage or added after the completion of the design process. Damping layers are applied to the structure as active or passive layers, and, depending on the problem considered, they may be implemented as free or constrained layers. Among the vibration control and reduction methods, the most efficient, easy, and commonly used one is the constrained-layer damping treatment. When this type of structure is subjected to cyclic bending, the damping layer is primarily subjected to shear strain due to the relative motion of the base and the constraining layers. Strong internal friction caused by this type of motion reduces the vibration amplitude for each bending cycle by dissipating the mechanical energy as heat.

A typical sandwich structure consists of two stiff face layers that carry the great portion of the bending load separated by a light inner core having an energy dissipating property. These structures find application as load carrying structural members due to their high stiffness-to-weight ratio in many engineering areas and especially in the field of aerospace. Therefore, a vast number of studies exist in the literature on the vibration analysis of viscoelastic sandwich structures. Earlier works can be traced back to 1950s to the study of Ross et al. [1], where the effects of layered shear treatments for simply supported plates were investigated. Sadasiva and Nakra [2] studied the unsymmetrically sectioned sandwich beams and plates with viscoelastic cores. Lu et al. [3] evaluated mechanical impedances for a sandwich plate with free boundary conditions by using the finite element method (FEM) and compared them with experimental results. Later, Johnson and Kienholz [4] studied the vibration and damping of sandwich ring and plate structures by using the modal strain energy method implemented in NASTRAN. One can find more recent studies, some of which are included in [5–15].

Viscoelastic polymeric materials have found great applications in engineering due to their high damping and energy dissipation properties. The dynamic modulus of elasticity and the loss factor of these materials show strong dependence on frequency and temperature. Therefore, it is not possible to obtain satisfying results, in terms of vibration damping, without taking proper account of the unique characteristics of these materials. There are several approaches to model the frequency dependence of the dynamic properties of viscoelastic materials, and the most commonly used

ones are the Golla–Hughes–McTavish (GHM) [16,17] and anelastic displacement field (ADF) methods [18]. In both of these methods, the complex modulus of the viscoelastic material is represented in terms of series of functions, where the fitting between the theoretical and experimental results is improved by increasing the number of terms considered. The obtained material properties are not valid for wide frequency ranges; besides, they are valid inside the frequency band, which is chosen for performing the fitting of master curves. On the other hand, fractional-order models of viscoelasticity obtained from the modification of conventional models such as Maxwell, Kelvin, and Zener exist in the literature [19,20], which overcome the drawbacks and limitations of GHM and ADF.

The differential quadrature method is a collocation scheme first introduced by Bellman et al. for the solution of nonlinear partial differential equations [21]. This method, in its first proposed form, produced ill-conditioned matrices for large systems, from which the weighting coefficients are obtained. This drawback was overcome with the introduction of the generalized differential quadrature method (GDQM) by Shu and Richards [22], which presents an explicit algebraic formula for the evaluation of weighting coefficients. Since then, GDQM has been efficiently applied to structural and vibration problems [23–26].

This study considers a modified version of the five-parameter fractional Zener model [20] in order to predict the viscoelastic behavior of the core layer. Governing equations together with the boundary conditions are obtained in terms of sectional moments and forces by using the principle of virtual work for the three-layered sandwich plate. Then, the resulting coupled partial differential equation system is solved by GDQM, which is a robust, accurate, and reliable numerical technique that can produce accurate results with considerably small number of grid points. Results are compared to already existing ones in the literature for three problems. Then, the effects of system parameters on the vibration and damping characteristic of a composite plate with a frequency-dependent viscoelastic core are investigated. The results are presented in graphical form in comparison with the results obtained with FEM. It is the first time that GDQM is applied to the vibration analysis of a sandwich structure, to the best of the authors' knowledge.

II. Equation of Motion

The assumptions used to derive the kinematic relations and the governing equations are as follows: 1) the viscoelastic core is represented by the complex modulus approach, 2) deformation through thickness is negligible, 3) transverse displacement does not change between the layers, 4) the plate deflection is small, and 5) there is no slip between the layers.

The geometry of the sandwich plate and the displacement of its layers is presented in Figs. 1 and 2, respectively.

The kinematic relations are derived from the geometry in Fig. 2 based on the first-order shear deformation theory (FSDT) as follows:

$$u^{(1)} = u_0 - \frac{h_2}{2}\varphi_2 - \left(z^{(1)} + \frac{h_1}{2}\right)\varphi_1 \tag{1}$$

$$v^{(1)} = v_0 - \frac{h_2}{2}\gamma_2 - \left(z^{(1)} + \frac{h_1}{2}\right)\gamma_1 \tag{2}$$

$$u^{(2)} = u_0 - z^{(2)}\varphi_2 \tag{3}$$

$$v^{(2)} = v_0 - z^{(2)}\gamma_2 \tag{4}$$

$$u^{(3)} = u_0 + \frac{h_2}{2}\varphi_2 + \left(\frac{h_3}{2} - z^{(3)}\right)\varphi_3 \tag{5}$$

$$v^{(3)} = v_0 + \frac{h_2}{2}\gamma_2 + \left(\frac{h_3}{2} - z^{(3)}\right)\gamma_3 \tag{6}$$

$$w^{(i)} = w, \qquad i = 1, 2, 3 \tag{7}$$

where φ_i and γ_i are the rotations of normals to midplane, $u^{(i)}$ and $v^{(i)}$ are the axial displacements, and $w^{(i)}$ is the transverse displacement of the ith layer. Also, u_0 and v_0 are the longitudinal displacements of the centroid of viscoelastic core. The strain–displacement relation for the linear vibrations of the sandwich plate is given by

$$\begin{Bmatrix} \varepsilon_{xx}^{(i)} \\ \varepsilon_{yy}^{(i)} \\ 2\varepsilon_{xy}^{(i)} \\ 2\varepsilon_{yz}^{(i)} \\ 2\varepsilon_{xz}^{(i)} \end{Bmatrix} = \begin{bmatrix} \partial/\partial x & 0 & 0 \\ 0 & \partial/\partial y & 0 \\ \partial/\partial y & \partial/\partial x & 0 \\ 0 & \partial/\partial z & \partial/\partial y \\ \partial/\partial z & 0 & \partial/\partial x \end{bmatrix} \begin{Bmatrix} u^{(i)} \\ v^{(i)} \\ w^{(i)} \end{Bmatrix}, \qquad i = 1, 2, 3 \tag{8}$$

The stress–strain relation for the composite-orthotropic base and constraining layers can be expressed as follows:

$$\begin{Bmatrix} \sigma_{xx}^{(i)} \\ \sigma_{yy}^{(i)} \\ \sigma_{xy}^{(i)} \\ \sigma_{yz}^{(i)} \\ \sigma_{xz}^{(i)} \end{Bmatrix} = \begin{bmatrix} \bar{Q}_{11}^{(i)} & \bar{Q}_{12}^{(i)} & \bar{Q}_{16}^{(i)} & 0 & 0 \\ \bar{Q}_{21}^{(i)} & \bar{Q}_{22}^{(i)} & \bar{Q}_{26}^{(i)} & 0 & 0 \\ \bar{Q}_{16}^{(i)} & \bar{Q}_{26}^{(i)} & \bar{Q}_{66}^{(i)} & 0 & 0 \\ 0 & 0 & 0 & \bar{Q}_{44}^{(i)} & \bar{Q}_{45}^{(i)} \\ 0 & 0 & 0 & \bar{Q}_{45}^{(i)} & \bar{Q}_{55}^{(i)} \end{bmatrix} \begin{Bmatrix} \varepsilon_{xx}^{(i)} \\ \varepsilon_{yy}^{(i)} \\ 2\varepsilon_{xy}^{(i)} \\ 2\varepsilon_{yz}^{(i)} \\ 2\varepsilon_{xz}^{(i)} \end{Bmatrix}, \qquad i = 1, 3 \tag{9}$$

where $\bar{Q}_{mn}^{(i)}$ are the transformed stiffness coefficients for the ith layer that can be expressed in terms of the lamina stiffness coefficients in principal material coordinates as given in the Appendix.

Since the viscoelastic core is isotropic with the Poisson's ratio assumed to be frequency independent, then the following stress–strain relation holds:

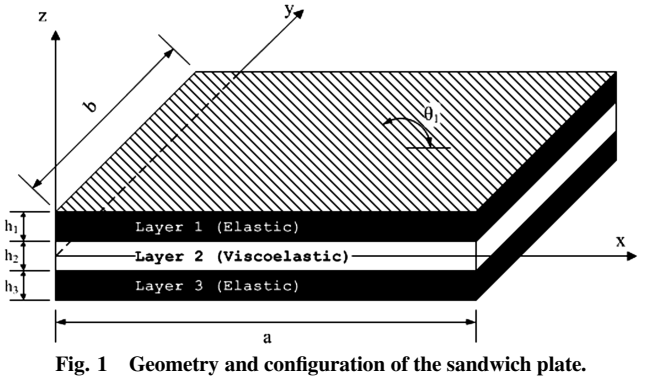

Fig. 1 Geometry and configuration of the sandwich plate.

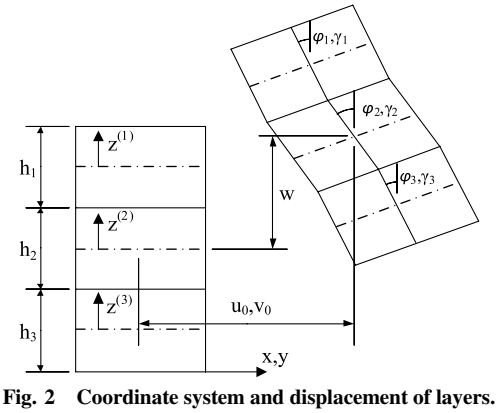

Fig. 2 Coordinate system and displacement of layers.

$$\begin{Bmatrix}\sigma_{xx}^{(2)}\\ \sigma_{yy}^{(2)}\\ \sigma_{xy}^{(2)}\\ \sigma_{yz}^{(2)}\\ \sigma_{xz}^{(2)}\end{Bmatrix}=\frac{E_2^*}{1-\nu_2^2}\begin{bmatrix}1 & \nu_2 & 0 & 0 & 0\\ \nu_2 & 1 & 0 & 0 & 0\\ 0 & 0 & 1-\nu_2 & 0 & 0\\ 0 & 0 & 0 & 1-\nu_2 & 0\\ 0 & 0 & 0 & 0 & 1-\nu_2\end{bmatrix}\begin{Bmatrix}\varepsilon_{xx}^{(2)}\\ \varepsilon_{yy}^{(2)}\\ \varepsilon_{xy}^{(2)}\\ \varepsilon_{yz}^{(2)}\\ \varepsilon_{xz}^{(2)}\end{Bmatrix} \tag{10}$$

where $E_2^*=E_2(1+i\eta_2)$ is the complex modulus of the viscoelastic core. For the free vibrations of the sandwich plate, Hamilton's principle can be expressed as follows:

$$\int_0^T(\delta U-\delta K)\,\mathrm{d}t=0 \tag{11}$$

where U and K correspond to the elastic strain energy and the kinetic energy, respectively. For the problem considered, Eq. (11) becomes

$$\sum_{i=1}^{3}\int_0^T\int_0^b\int_0^a\int_{-h_i/2}^{h_i/2}[\sigma_{xx}^{(i)}\delta\epsilon_{xx}^{(i)}+\sigma_{yy}^{(i)}\delta\epsilon_{yy}^{(i)}+2\sigma_{xy}^{(i)}\delta\epsilon_{xy}^{(i)}+2\sigma_{yz}^{(i)}\delta\epsilon_{yz}^{(i)}+2\sigma_{xz}^{(i)}\delta\epsilon_{xz}^{(i)}]\,\mathrm{d}z^{(i)}\,\mathrm{d}x\,\mathrm{d}y\,\mathrm{d}t-\sum_{i=1}^{3}\rho_i\int_0^T\int_0^b\int_0^a\int_{-h_i/2}^{h_i/2}\left[\frac{\partial u^{(i)}}{\partial t}\delta\frac{\partial u^{(i)}}{\partial t}+\frac{\partial v^{(i)}}{\partial t}\delta\frac{\partial v^{(i)}}{\partial t}+\frac{\partial w^{(i)}}{\partial t}\delta\frac{\partial w^{(i)}}{\partial t}\right]\mathrm{d}z^{(i)}\,\mathrm{d}x\,\mathrm{d}y\,\mathrm{d}t=0 \tag{12}$$

The governing equations in terms of sectional moments and forces are obtained from Eq. (12) by using the calculus of variations. These equations and related boundary conditions for the harmonic vibrations of the plate are presented in the Appendix.

III. Generalized Differential Quadrature Method

To approximate the derivatives of a function at a point, GDQM employs a weighted linear sum of the function values at all discrete points. The following relations hold for the uncoupled derivatives of a function $w(x,y)$ [25]:

$$\frac{\partial^p}{\partial x^p}w(x_i,y_j)=\sum_{k=1}^{N}c_{ik}^{(p)}w(x_k,y_j) \tag{13}$$

$$\frac{\partial^r}{\partial y^r}w(x_i,y_j)=\sum_{m=1}^{M}d_{jm}^{(r)}w(x_i,y_m) \tag{14}$$

where N and M are the total number of sampling points of the grid distribution in x and y directions, respectively. Also, $c_{ik}^{(p)}$ and $d_{jm}^{(r)}$ correspond to the weighting coefficients, which can be evaluated for the first-order derivatives as follows:

$$c_{ik}^{(1)}=\begin{cases}\dfrac{\bar{M}_x^{(1)}(x_i)}{(x_i-x_k)\bar{M}_x^{(1)}(x_k)} & \text{for } i\neq k \text{ and } i,k=1,2,\ldots N\\ -\sum_{s=1,s\neq i}^{N}c_{is}^{(1)} & \text{for } i=k \text{ and } i,k=1,2,\ldots N\end{cases} \tag{15}$$

$$d_{jm}^{(1)}=\begin{cases}\dfrac{\bar{M}_y^{(1)}(y_j)}{(y_j-y_m)\bar{M}_y^{(1)}(y_m)} & \text{for } j\neq m \text{ and } j,m=1,2,\ldots M\\ -\sum_{s=1,s\neq j}^{M}d_{js}^{(1)} & \text{for } j=m \text{ and } j,m=1,2,\ldots M\end{cases} \tag{16}$$

where the function $\bar{M}$ is given by

$$\bar{M}_x(x)=\prod_{s=1}^{N}(x-x_s),\qquad \bar{M}_y(y)=\prod_{s=1}^{M}(y-y_s) \tag{17}$$

The derivatives of $\bar{M}$ at discrete x_i and y_j points can be written as follows:

$$\bar{M}_x^{(1)}(x_i)=\prod_{s=1,s\neq i}^{N}(x_i-x_s),\qquad \bar{M}_y^{(1)}(y_j)=\prod_{s=1,s\neq j}^{M}(y_j-y_s) \tag{18}$$

The following recurrence relations hold for the weighting coefficients of higher-order derivatives:

$$c_{ik}^{(p)}=\begin{cases}p\left[c_{ii}^{(p-1)}c_{ik}^{(1)}-\dfrac{c_{ik}^{(p-1)}}{x_i-x_k}\right] & \text{for } i\neq k \text{ and } i,k=1,2,\ldots N\\ -\sum_{s=1,s\neq i}^{N}c_{is}^{(p)} & \text{for } i=k \text{ and } i,k=1,2,\ldots N\end{cases} \tag{19}$$

$$d_{jm}^{(r)}=\begin{cases}r\left[d_{jj}^{(r-1)}d_{jm}^{(1)}-\dfrac{d_{jm}^{(r-1)}}{y_j-y_m}\right] & \text{for } j\neq m \quad \text{and} \quad j,m=1,2,\ldots M\\ -\sum_{s=1,s\neq i}^{M}d_{js}^{(r)} & \text{for } j=m \quad \text{and} \quad j,m=1,2,\ldots M\end{cases} \tag{20}$$

The generalized differential quadrature (GDQ) formulation of the coupled derivative can also be given by

$$\frac{\partial^{p+r}}{\partial x^p\partial y^r}w(x_i,y_j)=\sum_{k=1}^{N}c_{ik}^{(p)}\sum_{m=1}^{M}d_{jm}^{(r)}w(x_k,y_m) \tag{21}$$

It is well known that the use of a grid distribution, which is denser on the boundaries, gives much better results when compared with a uniform distribution in GDQ analysis. Therefore, Chebyshev–Gauss–Labatto grid distribution is used to discretize the spatial coordinates:

$$x_i=\frac{a}{2}\left[1-\cos\left(\frac{i-1}{N-1}\pi\right)\right],\qquad y_j=\frac{b}{2}\left[1-\cos\left(\frac{j-1}{M-1}\pi\right)\right]$$
$$i=1,2,\ldots,N \quad \text{and} \quad j=1,2,\ldots,M \tag{22}$$

The grid distribution is presented in Fig. 3.

The open forms of governing equations and their GDQ representations are not presented here since these equations are quite large; however one can easily obtain them by using Eqs. (8–10) and (A12). The global assembling of the governing equations and the boundary conditions leads to the following set of linear equations [26]:

$$\begin{bmatrix}\mathbf{K}_{bb} & \mathbf{K}_{bd}\\ \mathbf{K}_{db} & \mathbf{K}_{dd}\end{bmatrix}\begin{Bmatrix}\boldsymbol{\delta}_b\\ \boldsymbol{\delta}_d\end{Bmatrix}=\omega^2\begin{bmatrix}0 & 0\\ 0 & \mathbf{M}_{dd}\end{bmatrix}\begin{Bmatrix}\boldsymbol{\delta}_b\\ \boldsymbol{\delta}_d\end{Bmatrix} \tag{23}$$

where the subscripts b and d stand for the degrees of freedom that belong to the boundary and the domain, respectively. Kinematic condensation of nondomain degrees of freedom can be performed as follows [24]:

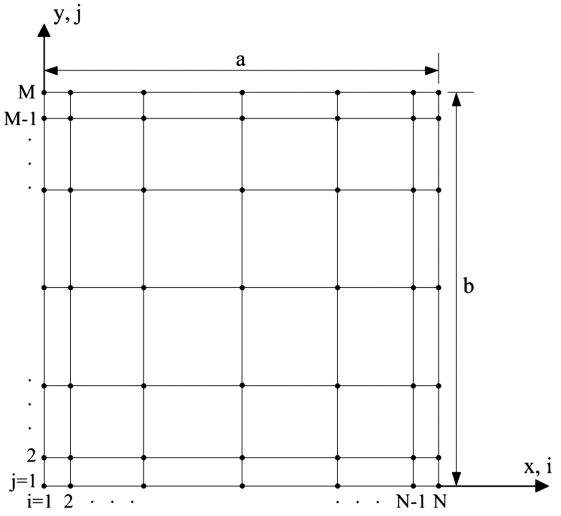

Fig. 3 Grid distribution.

$$(\mathbf{K}_{dd} - \mathbf{K}_{db}\mathbf{K}_{bb}^{-1}\mathbf{K}_{bd}) = \omega^2\mathbf{M}_{dd} \tag{24}$$

After solving Eq. (24) for the desired eigenpair, the displacements at the boundaries can also be obtained as follows:

$$\boldsymbol{\delta}_b = -\mathbf{K}_{bb}^{-1}\mathbf{K}_{bd}\boldsymbol{\delta}_d \tag{25}$$

In the solutions carried out, a symbolic calculation software package MATHEMATICA is used. The built-in function eigenvalues are used, which solves the generalized eigenvalue problem in Eq. (24) by the QZ algorithm.

IV. Five-Parameter Model

The dynamic modulus and the loss factor show strong dependency on the vibration frequency and temperature for the real polymeric materials. The five-parameter fractional model [20] is used in order to model the frequency dependency of the viscoelastic core:

$$G_2(\omega) = G_0 + G_0(d-1) \times \frac{\cos(\alpha\pi/2)(\omega\tau)^\alpha + \cos[(\alpha-\beta)\pi/2](\omega\tau)^{\alpha+\beta}}{1 + 2\cos(\beta\pi/2)(\omega\tau)^\beta + (\omega\tau)^{2\beta}} \tag{26}$$

where d is a ratio defined by $d = G_\infty/G_0$, G_0 is the static moduli, G_∞ is a parameter related to the high-frequency moduli, τ is the relaxation time, and α and β are the fractional-order time derivatives. Though it is more complicated, the five-parameter model is preferred to the classical four-parameter model since the latter is unable to capture the asymmetry of the loss factor peak.

It is not usually possible to obtain reliable experimental data over a broad frequency range at a desired temperature. Therefore, the experimental results for the shear modulus and loss factor are obtained for relatively narrow frequency ranges at different temperatures. Then, the effects of temperature and frequency are combined as a compound variable to obtain the master curves for the viscoelastic material, as follows:

$$G_2^*(\omega, T) = G_2^*(\omega f(T)) \tag{28}$$

Note that, the temperature–frequency equivalence principle in Eq. (28) holds for thermorheologically simple viscoelastic materials. The simple yet successful Arrhenius shift factor equation is used to model the relationship between temperature and frequency:

$$\log f(T) = T_A\left(\frac{1}{T} - \frac{1}{T_0}\right) \tag{29}$$

$$\eta_2(\omega) = \frac{(d-1)\{\sin(\pi\alpha/2)(\omega\tau)^\alpha + \sin[\pi(\alpha-\beta)/2](\omega\tau)^{\alpha+\beta}\}}{1 + (\omega\tau)^{2\beta} + 2\cos(\pi\beta/2)(\omega\tau)^\beta + (d-1)\{\cos(\pi\alpha/2)(\omega\tau)^\alpha + \cos[\pi(\alpha-\beta)/2](\omega\tau)^{\alpha+\beta}\}} \tag{27}$$

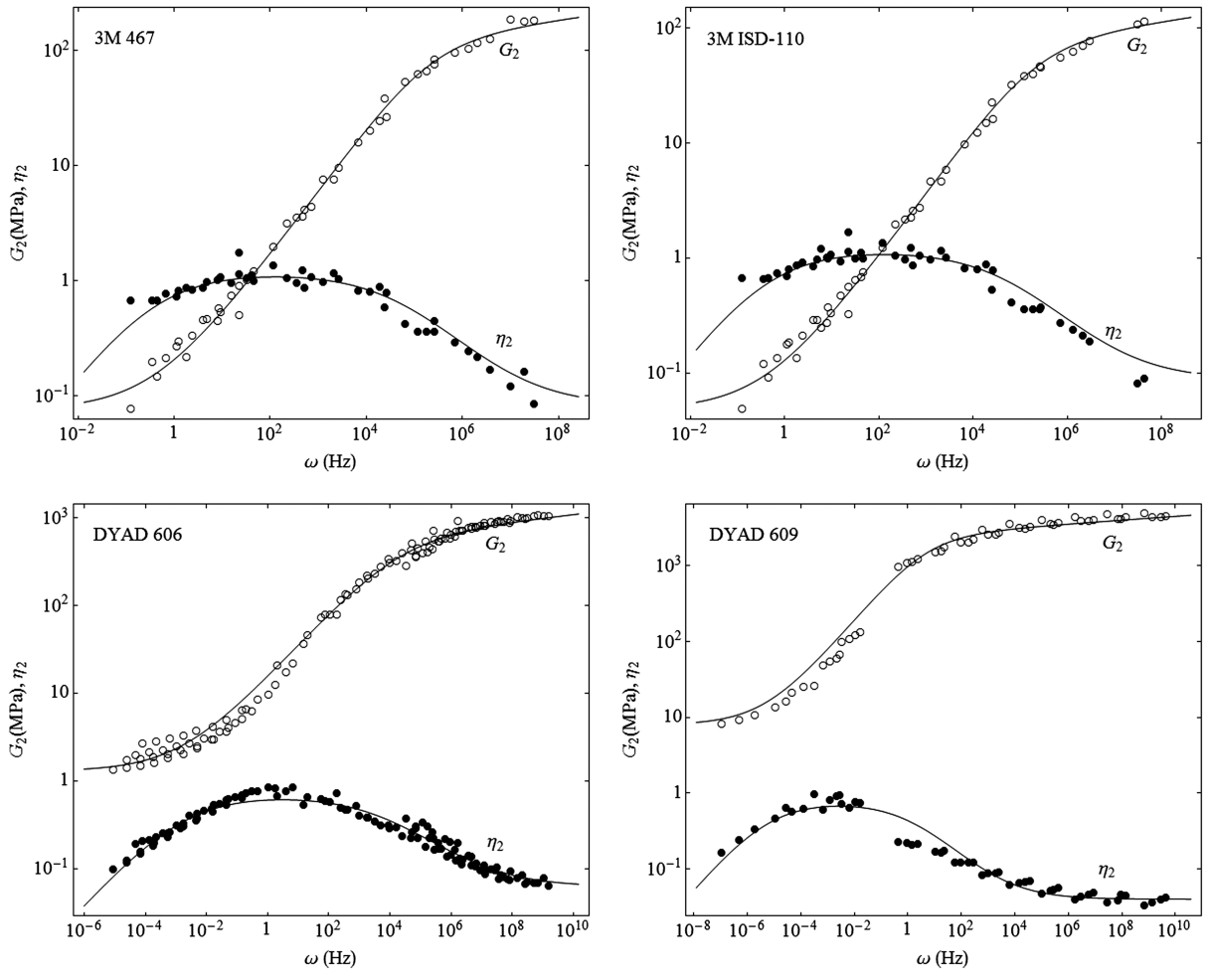

Fig. 4 Master curves of viscoelastic materials compared with experimental data ($T_0 = 21.1$ °C).

Table 1 Viscoelastic material properties

Material	G_0, Pa	d	α	β	τ, s	ρ_2, kg/m^3	T_A, °K
3M ISD-110	48×10^3	1685	0.550	0.494	7.73×10^{-6}	965	5050
3M 467	76×10^3	1753	0.553	0.501	7.98×10^{-6}	1080	5050
DYAD 606	1.29×10^6	499	0.383	0.343	8.66×10^{-5}	969	10450
DYAD 609	7.98×10^6	299	0.525	0.501	8.83	1107	10950
GE.SMRD [20]	5×10^6	36	0.605	0.554	2.09×10^{-4}	400	——
EAR C-1002 [20]	8×10^6	1570	0.566	0.558	7.23×10^{-10}	1300	——

where T_A is the activation temperature, T_0 is the reference temperature, and T is the actual temperature. The value of T_A is usually determined by minimizing the scatter in the logarithmic plots of the experimental data for the shear modulus and the loss factor versus frequency. In this study, T_A is evaluated by a program code, which minimizes the difference between the theoretical model and the experimental results.

The unknown material constants α, β, G_0, and G_∞ are obtained from the approximate low- and high-frequency behaviors of the dynamic moduli and the loss factor as described in [20]. On the other hand, the relaxation time τ is estimated by minimizing the difference between the experimental and theoretical data by using the least-squares method, as suggested by Galucio et al. [19]. The curve fitting process is applied to the experimental data presented in [27,28] for four commercial damping polymers. The first two are self-adhesive soft acrylic polymers from 3M, i.e., 3M ISD-110 and 3M 467. The other two are relatively stiff polyurethane polymers from Soundcoat, which are DYAD 606 and DYAD 609.

The master curves are presented in Fig. 4, and the numerical values of the optimized parameters for these four viscoelastic materials are presented in Table 1 together with two other damping polymers that already exist in the literature [20].

There is a good matching between the experimental and theoretical results, which shows that the five-parameter fractional model is quite successful in capturing the viscoelastic behavior. Also, note that the experimental data for DYAD 606 and DYAD 609 are given in the English system in [28], so they are converted to the SI system.

V. Results and Discussion

In this section, three sandwich plate problems that exist in the literature are considered to validate both the plate model and the solution technique. Then, a parametric analysis on the effects of system parameters on vibration and damping characteristics of a three-layered composite plate is carried out.

A. Validation

The first two cases consist of simply supported sandwich plates with elastic isotropic face layers and a viscoelastic core with constant material properties. These are hypothetical test problems, where the viscoelastic material properties are assumed to be frequency independent. The last case is a clamped composite plate with a frequency-dependent viscoelastic core. Geometric and material properties for the first example are given in Table 2.

This problem has attracted the attention of several researchers [4,6,8–12] and it has been used as a benchmark problem to test new plate theories and solution techniques. The vibration frequencies and the loss factors defined by Eq. (30) are presented for the first five modes in Table 3:

$$f = \sqrt{\mathrm{Re}(\omega_n^2)}, \qquad \eta = \frac{\mathrm{Im}(\omega_n^2)}{\mathrm{Re}(\omega_n^2)} \tag{30}$$

where ω_n is the nth complex natural frequency.

Navier's method is used in [6,8,9,12] for the solution of this eigenvalue problem. Though there are some differences between the

Table 2 Material properties and dimensions

Property	Dimension
Elastic layers (layers 1 and 3)	
Young's modulus	$E_1 = E_3 = 68.9$ GPa
Density	$\rho_1 = \rho_3 = 2740$ kg/m^3
Poisson's ratio	$\nu_1 = \nu_3 = 0.3$
Thickness	$h_1 = h_3 = 0.762$ mm
Viscoelastic layer (layer 2)	
Shear modulus	$G_2 = 0.896$ MPa
Density	$\rho_2 = 999$ kg/m^3
Poisson's ratio	$\nu_2 = 0.5$
Loss factor	$\eta_2 = 0.5$
Thickness	$h_2 = 0.254$ mm
Whole plate	
Length	$a = 0.348$ m, $b = 0.3048$ m

Table 4 Material properties and dimensions

Property	Dimension
Elastic layers (layers 1 and 3)	
Young's modulus	$E_1 = E_3 = 207$ GPa
Density	$\rho_1 = \rho_3 = 7800$ kg/m^3
Poisson's ratio	$\nu_1 = \nu_3 = 0.334$
Thickness	$h_1 = h_3 = 5$ mm
Viscoelastic layer (layer 2)	
Shear modulus	$G_2 = 4$ MPa
Density	$\rho_2 = 2000$ kg/m^3
Poisson's ratio	$\nu_2 = 0.3$
Loss factor	$\eta_2 = 0.38$
Thickness	$h_2 = 5$ mm
Whole plate	
Length	$a = b = 0.4$ m

Table 3 Natural frequencies and loss factors ($N = 30$, $M = 26$)

	Frequency, Hz					Loss factor				
Analysis	First	Second	Third	Fourth	Fifth	First	Second	Third	Fourth	Fifth
Proposed	57.96	113.80	129.36	177.11	194.72	0.1706	0.1933	0.1927	0.1730	0.1705
Reference [4]	57.4	113.2	129.3	179.3	196.0	0.176	0.188	0.188	0.153	0.153
Reference [6]	60.2	115.2	130.2	178.5	195.4	0.190	0.203	0.199	0.181	0.174
Reference [8]	60.2	115.2	130.4	178.4	195.4	0.190	0.203	0.199	0.181	0.174
Reference [9]	60.1	115.0	130.2	178.1	195.1	0.192	0.203	0.198	0.179	0.172
Reference [10]	56.9	111.9	127.5	174.9	193.1	0.180	0.190	0.187	0.164	0.158
Reference [11]	58.69	113.75	129.16	175.46	193.79	0.201	0.211	0.208	0.189	0.183
Reference [12]	60.24	115.22	130.43	178.46	195.42	0.1901	0.2034	0.1991	0.1806	0.1737

Table 5 Natural frequencies and loss factors ($N = 30, M = 30$)

	Frequency, rad/s				Loss factor, %			
Analysis	First	Second	Third	Fourth	First	Second	Third	Fourth
Proposed	970.10	2340.76	2340.76	3700.19	4.391	1.919	1.919	1.232
Reference [5]	975.17	2350.79	2350.79	3725.33	4.431	1.918	1.918	1.224
Reference [7]	974.91	2350.80	2350.80	3725.60	4.386	1.911	1.911	1.221
Reference [11]	972.89	2346.45	2346.45	3711.90	4.4	1.9	1.9	1.2

plate models used in these studies, the results show little variation probably due to the same shape functions used for the displacements. On the other hand, the natural frequencies and loss factors are obtained with FEM analyses in [4,10,11].

The properties of the second plate are given in Table 4 and the results for the first four natural frequencies and loss factors are presented in Table 5.

The tables show good agreement between the results obtained with GDQM and the already existing ones. It is common to model the base and constraining layers with Kirchhoff plate theory [5,8–10,12] in order to simplify the problem by decreasing the number of degrees of freedom. As a result, the neglected transverse shear strain results in an overprediction of the natural frequencies. In this study, all layers are modeled with Mindlin plate theory and therefore the natural frequencies obtained are generally lower when compared with the results of other studies.

The convergence of the loss factors in example 2 for the first four modes with increasing number of terms considered is presented in Fig. 5.

The third example is a clamped seven-layered composite plate having carbon fiber face layers and a viscoelastic core made of 3M ISD 112 damping polymer. The stacking sequence of the sandwich plate is 0/90/45/core/45/90/0 and the material properties and dimensions are as given in Table 6.

This problem was considered by Araujo et al. to identify the unknown parameters of fractional-order viscoelastic models [29]. In their study, the core layer is modeled with a higher-order shear deformation theory (HSDT) and the face layers are modeled with FSDT. Also, an eight-node serendipity plate element with 13 mechanical degrees of freedom per node was used for the FEM analysis of this problem. The shear modulus and loss factor of the viscoelastic core, for the frequency range $f = 5 \ldots 1600$ Hz, are as follows [29,30]:

$$G_2 = 4.759 - \frac{0.9266}{0.1918 + 0.0005148f} + 2.405(0.1918 + 0.0005148f)^2$$
$$\eta_2 = 1.385 - 0.03673(0.01 + 0.0006306f) - \frac{0.01342}{0.01 + 0.0006306f} \tag{31}$$

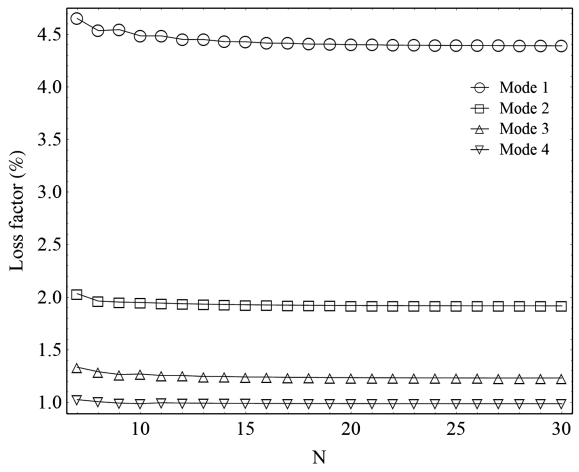

Fig. 5 Convergence of the loss factor with *N*.

Since the core material is frequency dependent for this problem, Eq. (24) is nonlinear and it is necessary to use an iterative approach to solve this eigenvalue problem. Therefore, an initial guess for the desired mode is made and the problem is solved for the corresponding material properties of the viscoelastic core. Then, the numerical result obtained for the natural frequency of the sandwich plate is used as next guess. The iteration is repeated until the vibration frequency converges to a value [13,29]:

$$\frac{\|f_n^{i+1} - f_n^i\|}{f_n^i} \leq \xi \tag{32}$$

where ξ is the error tolerance and f_n^i is the nth natural frequency at ith iteration. The results for the first 12 natural frequencies and loss factors are presented in Table 7 for $\xi = 0.0001$.

We also solved this problem with a currently developed FEM, where the mass and stiffness matrices are derived by considering classical plate theory for the base and the constraining layers and FSDT for the core layer [31]. A four-node quadrilateral plate element with seven degrees of freedom per node is used in the calculations [31]. The results of this FEM analysis are given in the last two columns of Table 6. Also, GDQM estimations for the natural frequencies and loss factors when the core layer is modeled with HSDT as in [29] are presented in Table 7.

There is some discrepancy between the results of [29] and the recent study especially for the higher modes. Since there is a good agreement between different models and solution techniques of the present study, we conclude that the reason for this inconsistency is most probably due to the coarse mesh used in [29]. Results also show that the additional computational cost of using HSDT instead of FSDT in the modeling of the core layer is not justified since there is almost no difference between the frequencies and loss factors obtained with these two theories.

Comparison of GDQ and FEMs, in terms of variation of the relative error and the CPU time with respect to the number of nodes considered, is presented in Fig. 6 for the first natural frequency of the last example.

Figure 6 shows that GDQM requires more CPU time to solve the problem than FEM, for the same number of nodes considered. This is mainly due to the fact that it requires more effort to solve the dense and asymmetric stiffness matrices produced by GDQ method compared to the sparse and symmetric stiffness matrices obtained with FEM. Nevertheless, the computational effort required to achieve

Table 6 Properties of the composite plate

Property	Dimension
Carbon fiber layers (layers 1 and 3)	
Young's modulus	$E_{11} = 130.8$ GPa, $E_{22} = 10.6$ GPa
Shear modulus	$G_{12} = 5.6$ GPa, $G_{13} = 4.2$ GPa, $G_{23} = 3.0$ GPa
Density	$\rho_1 = \rho_3 = 1543$ kg/m^3
Poisson's ratio	$\nu_{12} = 0.36$
Thickness	$h_1 = h_3 = 1.5$ mm
Viscoelastic layer (layer 2)	
Shear modulus	$G_2 = G_2(\omega)$
Density	$\rho_2 = 1000$ kg/m^3
Poisson's ratio	$\nu_2 = 0.49$
Loss factor	$\eta_2 = \eta_2(\omega)$
Thickness	$h_2 = 2.5$ mm
Whole plate	
Length	$a = 0.3$ m, $b = 0.2$ m

Table 7 Natural frequencies and loss factors ($N = 30, M = 20$)

	FEM [29]		GDQM[a]		GDQM[b]		FEM[c]	
Mode	f, Hz	η, %	f, Hz	η, %	f, Hz	η, %	f, Hz	η, %
1	211.72	46.58	216.4971	50.6700	216.4971	50.6700	217.1197	50.7598
2	382.63	41.87	375.0547	49.8528	375.0547	49.8527	376.2565	49.9284
3	473.22	42.52	469.5071	48.2577	469.5071	48.2576	472.8345	48.1989
4	630.85	39.41	580.8453	51.8697	580.8453	51.8696	583.7805	51.8075
5	674.83	31.93	635.8137	40.9737	635.8137	40.9737	639.0632	41.0070
6	876.43	39.59	801.5226	48.3322	801.5225	48.3321	805.5127	48.0869
7	963.66	32.92	828.7563	44.6736	828.7562	44.6735	840.2958	44.3153
8	995.54	31.43	923.4911	42.5272	923.4910	42.5272	932.2388	42.3802
9	1080.30	33.41	969.8134	38.3451	969.8133	38.3451	978.6948	38.2968
10	1393.95	30.16	1054.6749	47.4708	1054.6747	47.4707	1061.5413	47.1812
11	1440.67	33.90	1210.4852	37.9273	1210.4849	37.9271	1218.9995	37.3892
12	1461.00	27.51	1298.7898	38.3266	1298.7897	38.3265	1317.9316	38.3406

[a]Core modeled with FSDT.
[b]Core modeled with HSDT.
[c]FEM results of the present study with a 30 × 20 mesh.

a desired accuracy is smaller for GDQ method since it shows better convergence characteristics when compared to FEM. Similar findings have also been reported in [24], where the CPU time and accuracy are compared between GDQM and commercial FEM software.

B. Parametric Analysis

The effect of geometric properties as well as the choice of core material on damping and vibration characteristics of a rectangular sandwich plate with clamped boundary conditions will be analyzed in this section. The material for the composite base and constraining layers are selected as carbon fiber reinforced plastic (CFRP) with the material properties given in Table 8. The shear modulus and loss factor of the viscoelastic core are calculated from Eqs. (26) and (27) together with the data in Table 1. The iterative approach described for the third example is used with the same error tolerance, $\xi = 0.0001$.

Though the loss factors of elastic face layers are usually quite small when compared with the loss factor of the viscoelastic material, it may not be safe to omit them since the contribution to the total loss factor of the structure is proportional with the stored strain energy [32]. The loss factors of CFRPs usually vary in the range $0.001 < \eta < 0.005$ [33]; therefore, an approximate average value $\eta = 0.003$ is attributed to the CFRP material in order to include the damping contribution of the face layers. Also, to be on the safe side, the results obtained with GDQM are compared with the results of the recent FEM model with a 15 × 20 mesh.

The effect of lamination angle of the constraining layer on the fundamental frequency and loss factor is presented in Fig. 7. The plate section is geometrically symmetrical and the base layer is held at a constant lamination angle, $\theta_3 = 0$. Figure 7 shows that the frequency and the loss factor are maximized for a symmetric layup 0/core/0. The loss factor has its greatest values when the core material is a damping polymer from 3M. Also, the maximum values of the frequency and the minimum values of the loss factor belong to a DYAD 609 core. An interesting point observed is that the loss factor of the sandwich plate is almost constant with the lamination angle of the constraining layer, when the core material is EAR C-1002.

The effect of face layer thicknesses on the vibration and damping characteristics of the sandwich plate is shown in Fig. 8, where the base and constraining layers are taken of equal height. As a result of increasing sectional stiffness, the frequency increases with h_1 and h_3 for all types of the core material as expected. On the other hand, the loss factor has a global maximum at a specific thickness of the face layers for each core material. Again, the viscoelastic materials from 3M show the best damping characteristics for this plate configuration. Also, note that the deviation of predicted frequencies between FEM and GDQM solutions increases with increasing thicknesses, h_1 and h_3. This is quite natural since the shear stresses ignored in the FEM model dominate as the thicknesses of the face layers increase and the thin plate model starts to fail.

The effect of core thickness on the natural frequency and modal loss factor is presented in Fig. 9. The frequencies decrease with increasing core thickness as a result of the decreasing ratio of the sectional stiffness to mass for the relatively soft damping materials, i.e., 3M ISD-110, 3M 467, and EAR C-1002. For the other three stiff materials, this effect is vice versa. The modal loss factor tends to increase with core thickness as expected. As can be deduced from the figure, the best choices of core material in order to achieve better

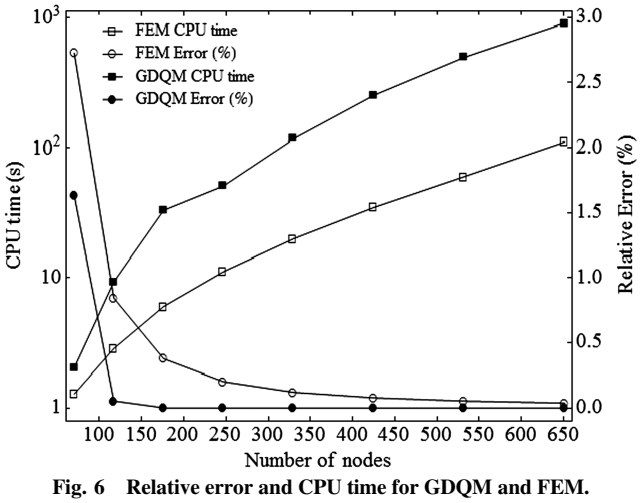

Fig. 6 Relative error and CPU time for GDQM and FEM.

Table 8 Properties of the composite plate

Property	Dimension
CFRP composite layers (layers 1 and 3)	
Young's modulus	$E_{11} = 138.6$ GPa, $E_{22} = 8.27$ GPa
Shear modulus	$G_{12} = G_{13} = 4.96$ GPa, $G_{23} = 4.12$ GPa
Density	$\rho_1 = \rho_3 = 1824$ kg/m^3
Poisson's ratio	$\nu_{12} = 0.26$
Thickness	Variable
Viscoelastic layer (layer 2)	
Shear modulus	$G_2 = G_2(\omega)$
Density	ρ_2 (Table 1)
Poisson's ratio	$\nu_2 = 0.5$
Loss factor	$\eta_2 = \eta_2(\omega)$
Thickness	Variable
Whole plate	
Length	$a = 0.3$ m, $b = 0.4$ m

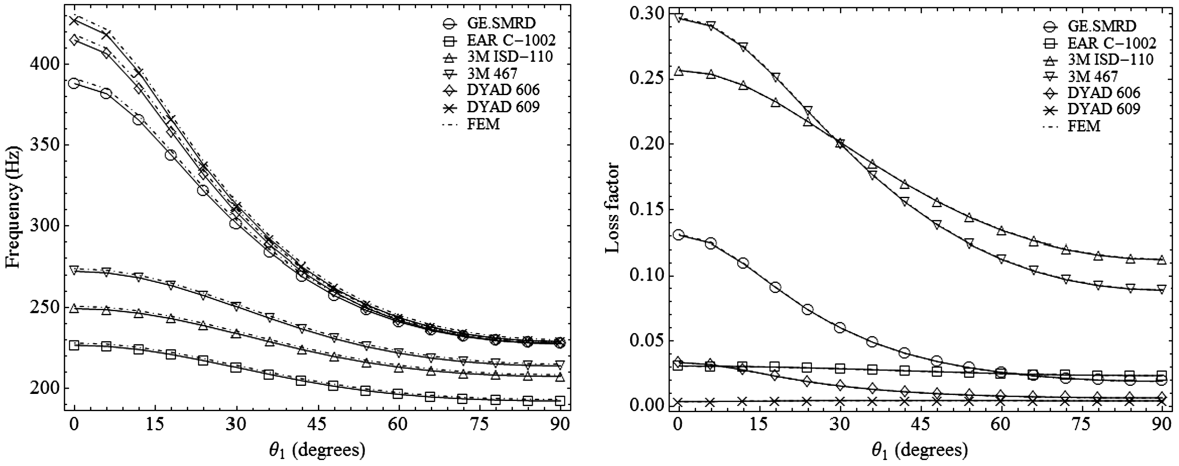

Fig. 7 Variation of the frequency and loss factor with θ_1 ($h_1 = 2$ mm, $h_2 = 0.2$ mm, $h_3 = 2$ mm).

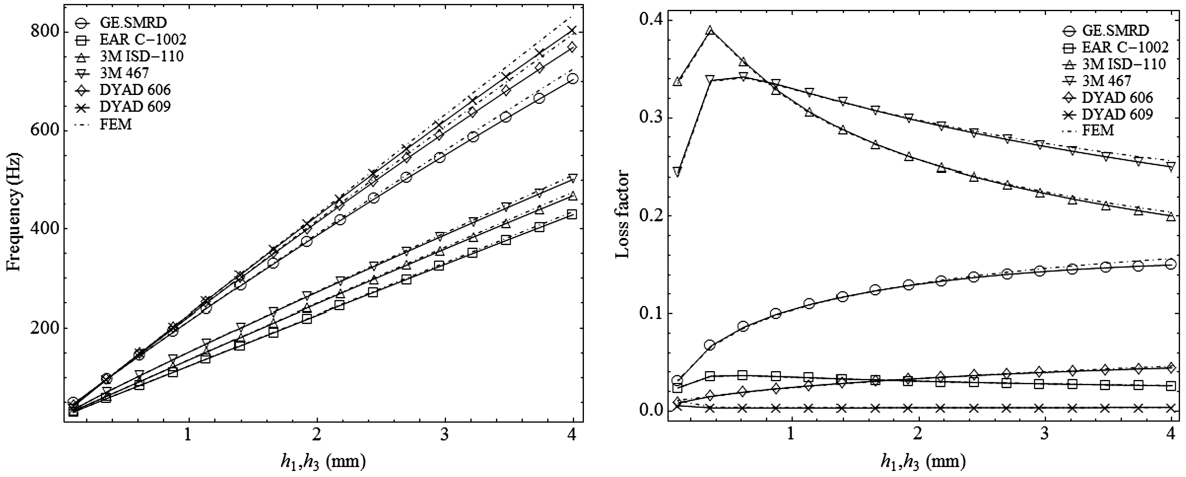

Fig. 8 Variation of the frequency and loss factor with $h_1 = h_3$ ($h_2 = 0.2$ mm, $\theta_1 = 0$, $\theta_3 = 0$).

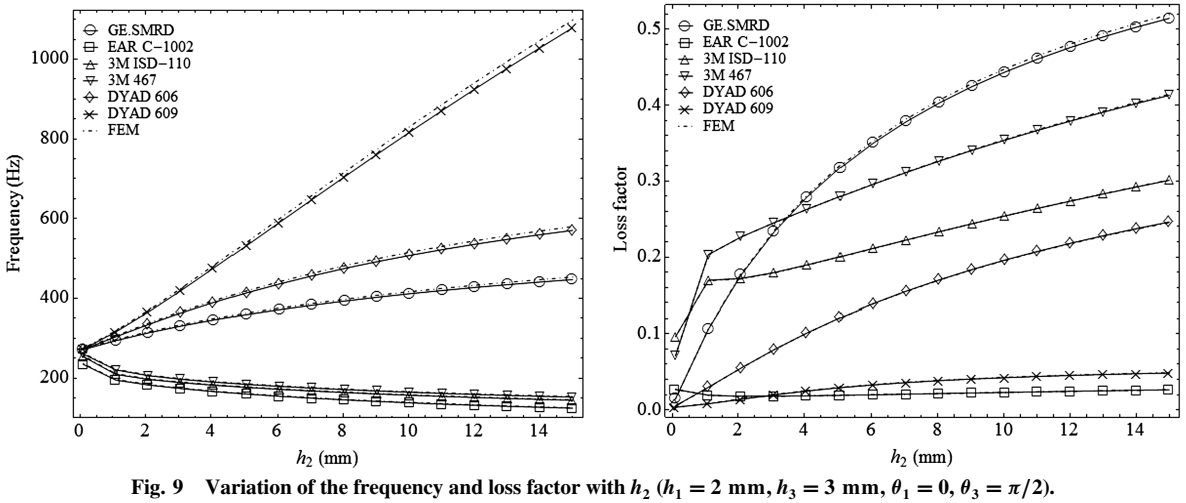

Fig. 9 Variation of the frequency and loss factor with h_2 ($h_1 = 2$ mm, $h_3 = 3$ mm, $\theta_1 = 0$, $\theta_3 = \pi/2$).

damping results are 3M ISD-110 and 3M 467, for smaller values of h_2. For the larger thicknesses of the core layer, GE.SMRD seems to be the best choice.

Lastly, the effect of the location of the viscoelastic core inside the plate is shown in Fig. 10. The maximum values of the modal loss factor correspond to symmetrical configurations, where $h_1 = h_3$, for all choices of the core material. This result is expected since the core experiences the greatest magnitudes of shear stress for symmetrical configurations. On the other hand, this effect seems to be vice versa for the frequency for most of the core materials, i.e., the minimum

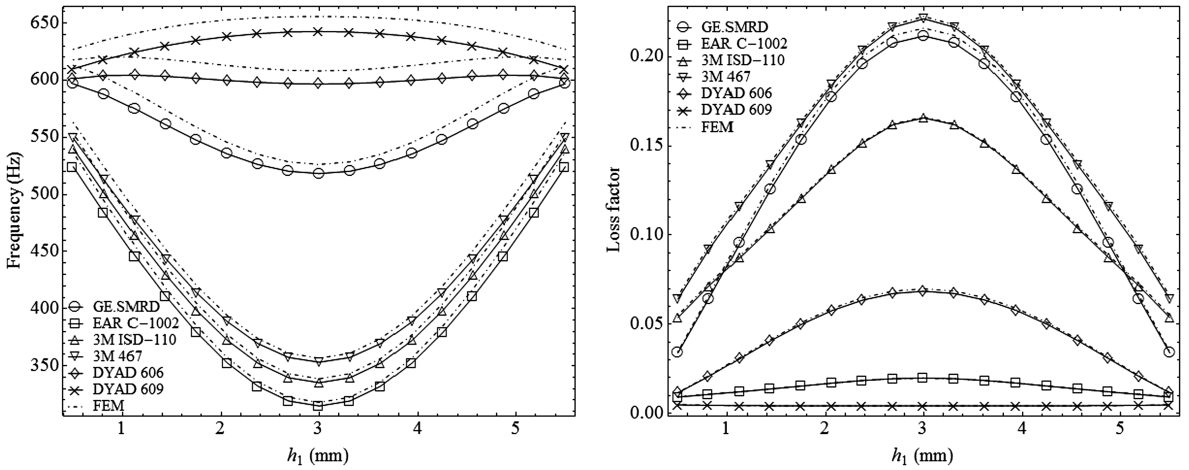

Fig. 10 Variation of the frequency and loss factor with the location of core ($h_1 + h_3 = 6$ mm, $h_2 = 0.4$ mm, $\theta_1 = 0$, $\theta_3 = 0$).

value of the natural frequency corresponds to the symmetrical case and a deformation of symmetry results in an increase due to increasing rigidity. The best choice, in terms of vibration damping, seems to be 3M 467 for all possible variations of the location of viscoelastic core. The matching between the results obtained with FEM and GDQM is quite satisfactory for the loss factor; however, there is some discrepancy between the results obtained with these two methods for the frequency, especially for the stiff core materials and asymmetrical plate sections.

VI. Conclusions

In this study, the fundamental frequencies and loss factors of composite sandwich plates with viscoelastic cores are calculated by using GDQM, for the first time. The results obtained with GDQM are compared with the results of other studies in order to verify the plate model and the solution technique. The five-parameter fractional Zener model is used to take into account the frequency dependency of the core layer. The unknown material parameters of the polymeric damping materials considered in the core layer are evaluated from the experimental results that exist in the literature. It is observed that the correlation between the theoretical and experimental results is exceptionally good. The effects of system parameters such as lamination angle, thicknesses of layers, and location of the core layer on the frequencies and loss factors are investigated for different core materials for clamped plates with CFRP face layers. It is found that the core material that provides the highest damping depends on the geometrical properties of the plate. Therefore, finding a global optimum of the system parameters to maximize the modal loss factor would be a challenging multiparameter optimization problem, which can be carried out as a future study. On the other hand, results have shown that symmetrical layups, where the material and geometrical properties of the constraining and base layers are identical, present better damping results when compared with the nonsymmetrical layups.

The eigenproblem is also solved with FEM by using a four-node quadrilateral plate element, where the face layers are modeled with Kirchhoff theory. The results of both GDQM and FEM are compared and presented graphically, and a good agreement between these two methods is observed. This study reveals that GDQM can be efficiently used as an accurate and robust alternative to FEM in the vibration analysis of sandwich plates.

Appendix: Governing Equations and Boundary Conditions

The relation between transformed stiffness coefficients and the lamina stiffness coefficients in principal material coordinates is as follows:

$$
\begin{aligned}
\bar{Q}_{11}^{(i)} &= Q_{11}\cos^4\theta_i + 2(Q_{12} + 2Q_{66})\sin^2\theta_i\cos^2\theta_i + Q_{22}\sin^4\theta_i \\
\bar{Q}_{12}^{(i)} &= (Q_{11} + Q_{22} - 4Q_{66})\sin^2\theta_i\cos^2\theta_i + Q_{12}(\sin^4\theta_i + \cos^4\theta_i) \\
\bar{Q}_{22}^{(i)} &= Q_{11}\sin^4\theta_i + 2(Q_{12} + 2Q_{66})\sin^2\theta_i\cos^2\theta_i + Q_{22}\cos^4\theta_i \\
\bar{Q}_{16}^{(i)} &= (Q_{11} - Q_{12} - 2Q_{66})\sin\theta_i\cos^3\theta_i \\
&\quad + (Q_{12} - Q_{22} + 2Q_{66})\sin^3\theta_i\cos\theta_i \\
\bar{Q}_{26}^{(i)} &= (Q_{11} - Q_{12} - 2Q_{66})\sin^3\theta_i\cos\theta_i \\
&\quad + (Q_{12} - Q_{22} + 2Q_{66})\sin\theta_i\cos^3\theta_i \\
\bar{Q}_{66}^{(i)} &= (Q_{11} + Q_{22} - 2Q_{12} - 2Q_{66})\sin^2\theta_i\cos^2\theta_i \\
&\quad + Q_{66}(\sin^4\theta_i + \cos^4\theta_i) \\
\bar{Q}_{44}^{(i)} &= Q_{44}\cos^2\theta_i + Q_{55}\sin^2\theta_i \\
\bar{Q}_{45}^{(i)} &= (Q_{55} - Q_{44})\cos\theta_i\sin\theta_i \\
\bar{Q}_{55}^{(i)} &= Q_{55}\cos^2\theta_i + Q_{44}\sin^2\theta_i
\end{aligned}
\tag{A1}
$$

where θ_i is the angle of lamination of the ith layer and Q_{mn} are related to the engineering constants as follows:

$$
Q_{11} = \frac{E_1}{1-\nu_{12}\nu_{21}}, \quad Q_{12} = \frac{\nu_{12}E_2}{1-\nu_{12}\nu_{21}}, \quad Q_{22} = \frac{E_2}{1-\nu_{12}\nu_{21}},
$$
$$
Q_{66} = G_{12}, \quad Q_{44} = G_{23}, \quad Q_{55} = G_{13}, \quad \nu_{21} = \frac{E_2\nu_{12}}{E_1} \tag{A2}
$$

The governing equations are obtained as follows:

$$
\begin{aligned}
&\frac{\partial N_{xx}^{(1)}}{\partial x} + \frac{\partial N_{xx}^{(2)}}{\partial x} + \frac{\partial N_{xx}^{(3)}}{\partial x} + \frac{\partial N_{xy}^{(1)}}{\partial y} + \frac{\partial N_{xy}^{(2)}}{\partial y} + \frac{\partial N_{xy}^{(3)}}{\partial y} \\
&\quad = \omega^2\left[\frac{1}{2}h_1^2\rho_1\varphi_1 + \frac{1}{2}h_2(h_1\rho_1 - h_3\rho_3)\varphi_2 - \frac{1}{2}h_3^2\rho_3\varphi_3\right. \\
&\qquad \left. - (h_1\rho_1 + h_2\rho_2 + h_3\rho_3)u_0\right]
\end{aligned}
\tag{A3}
$$

$$
\begin{aligned}
&\frac{\partial N_{yy}^{(1)}}{\partial y} + \frac{\partial N_{yy}^{(2)}}{\partial y} + \frac{\partial N_{yy}^{(3)}}{\partial y} + \frac{\partial N_{xy}^{(1)}}{\partial x} + \frac{\partial N_{xy}^{(2)}}{\partial x} + \frac{\partial N_{xy}^{(3)}}{\partial x} \\
&\quad = \omega^2\left[\frac{1}{2}h_1^2\rho_1\gamma_1 + \frac{1}{2}h_2(h_1\rho_1 - h_3\rho_3)\gamma_2 - \frac{1}{2}h_3^2\rho_3\gamma_3\right. \\
&\qquad \left. - (h_1\rho_1 + h_2\rho_2 + h_3\rho_3)v_0\right]
\end{aligned}
\tag{A4}
$$

$$\frac{\partial N_{xz}^{(1)}}{\partial x}+\frac{\partial N_{xz}^{(2)}}{\partial x}+\frac{\partial N_{xz}^{(3)}}{\partial x}+\frac{\partial N_{yz}^{(1)}}{\partial y}+\frac{\partial N_{yz}^{(2)}}{\partial y}+\frac{\partial N_{yz}^{(3)}}{\partial y}$$
$$=-\omega^2(h_1\rho_1+h_2\rho_2+h_3\rho_3)w \tag{A5}$$

$$\frac{1}{2}h_1\left(\frac{\partial N_{xx}^{(1)}}{\partial x}+\frac{\partial N_{xy}^{(1)}}{\partial y}\right)+\frac{\partial M_{xx}^{(1)}}{\partial x}+\frac{\partial M_{xy}^{(1)}}{\partial y}-N_{xz}^{(1)}$$
$$=\frac{1}{12}h_1^2\rho_1\omega^2(4h_1\varphi_1+3h_2\varphi_2-6u_0) \tag{A6}$$

$$\frac{1}{2}h_2\left(\frac{\partial N_{xx}^{(1)}}{\partial x}+\frac{\partial N_{xy}^{(1)}}{\partial y}-\frac{\partial N_{xx}^{(3)}}{\partial x}-\frac{\partial N_{xy}^{(3)}}{\partial y}\right)+\frac{\partial M_{xx}^{(2)}}{\partial x}+\frac{\partial M_{xy}^{(2)}}{\partial y}-N_{xz}^{(2)}$$
$$=\frac{1}{12}h_2\omega^2[(6h_3\rho_3-6h_1\rho_1)u_0+3h_1^2\rho_1\varphi_1+h_2(3h_1\rho_1+h_2\rho_2+3h_3\rho_3)\varphi_2+3h_3^2\rho_3\varphi_3] \tag{A7}$$

$$\frac{\partial M_{xx}^{(3)}}{\partial x}+\frac{\partial M_{xy}^{(3)}}{\partial y}-\frac{1}{2}h_3\left(\frac{\partial N_{xx}^{(3)}}{\partial x}+\frac{\partial N_{xy}^{(3)}}{\partial y}\right)-N_{xz}^{(3)}$$
$$=\frac{1}{12}h_3^2\rho_3\omega^2(6u_0+4h_3\varphi_3+3h_2\varphi_2) \tag{A8}$$

$$\frac{1}{2}h_1\left(\frac{\partial N_{yy}^{(1)}}{\partial y}+\frac{\partial N_{xy}^{(1)}}{\partial x}\right)+\frac{\partial M_{yy}^{(1)}}{\partial y}+\frac{\partial M_{xy}^{(1)}}{\partial x}-N_{yz}^{(1)}$$
$$=\frac{1}{12}h_1^2\rho_1\omega^2(4h_1\gamma_1+3h_2\gamma_2-6v_0) \tag{A9}$$

$$\frac{1}{2}h_2\left(\frac{\partial N_{yy}^{(1)}}{\partial y}+\frac{\partial N_{xy}^{(1)}}{\partial x}-\frac{\partial N_{yy}^{(3)}}{\partial y}-\frac{\partial N_{xy}^{(3)}}{\partial x}\right)+\frac{\partial M_{yy}^{(2)}}{\partial y}+\frac{\partial M_{xy}^{(2)}}{\partial x}-N_{yz}^{(2)}$$
$$=\frac{1}{12}h_2\omega^2[(6h_3\rho_3-6h_1\rho_1)v_0+3h_1^2\rho_1\gamma_1+h_2(3h_1\rho_1+h_2\rho_2+3h_3\rho_3)\gamma_2+3h_3^2\rho_3\gamma_3] \tag{A10}$$

$$\frac{\partial M_{yy}^{(3)}}{\partial y}+\frac{\partial M_{xy}^{(3)}}{\partial x}-\frac{1}{2}h_3\left(\frac{\partial N_{yy}^{(3)}}{\partial y}+\frac{\partial N_{xy}^{(3)}}{\partial x}\right)-N_{yz}^{(3)}$$
$$=\frac{1}{12}h_3^2\rho_3\omega^2(6v_0+4h_3\gamma_3+3h_2\gamma_2) \tag{A11}$$

The sectional moment and forces are obtained from the following equations:

$$N_{mn}^{(i)}=\int_{-h_i/2}^{h_i/2}\sigma_{mn}^{(i)}\,\mathrm{d}z^{(i)}$$
$$M_{mn}^{(i)}=\int_{-h_i/2}^{h_i/2}z^{(i)}\sigma_{mn}^{(i)}\,\mathrm{d}z^{(i)}$$
$$i=1,2,3 \tag{A12}$$

And the boundary conditions are evaluated as follows:

$$(N_{xx}^{(1)}+N_{xx}^{(2)}+N_{xx}^{(3)})\delta u_0|_{x=0}^{a}=0$$
$$(N_{xy}^{(1)}+N_{xy}^{(2)}+N_{xy}^{(3)})\delta v_0|_{x=0}^{a}=0$$
$$(N_{xz}^{(1)}+N_{xz}^{(2)}+N_{xz}^{(3)})\delta w|_{x=0}^{a}=0$$
$$\left(M_{xx}^{(1)}+\frac{1}{2}h_1N_{xx}^{(1)}\right)\delta\varphi_1|_{x=0}^{a}=0$$
$$\left[M_{xx}^{(2)}+\frac{1}{2}h_2(N_{xx}^{(1)}-N_{xx}^{(3)})\right]\delta\varphi_2|_{x=0}^{a}=0$$
$$\left(M_{xx}^{(3)}-\frac{1}{2}h_3N_{xx}^{(3)}\right)\delta\varphi_3|_{x=0}^{a}=0$$
$$\left(M_{xy}^{(1)}+\frac{1}{2}h_1N_{xy}^{(1)}\right)\delta\gamma_1|_{x=0}^{a}=0$$
$$\left[M_{xy}^{(2)}+\frac{1}{2}h_2(N_{xy}^{(1)}-N_{xy}^{(3)})\right]\delta\gamma_2|_{x=0}^{a}=0$$
$$\left(M_{xy}^{(3)}-\frac{1}{2}h_3N_{xy}^{(3)}\right)\delta\gamma_3|_{x=0}^{a}=0 \tag{A13}$$

$$(N_{xy}^{(1)}+N_{xy}^{(2)}+N_{xy}^{(3)})\delta u_0|_{y=0}^{b}=0$$
$$(N_{yy}^{(1)}+N_{yy}^{(2)}+N_{yy}^{(3)})\delta v_0|_{y=0}^{b}=0$$
$$(N_{yz}^{(1)}+N_{yz}^{(2)}+N_{yz}^{(3)})\delta w|_{y=0}^{b}=0$$
$$\left(M_{xy}^{(1)}+\frac{1}{2}h_1N_{xy}^{(1)}\right)\delta\varphi_1|_{y=0}^{b}=0$$
$$\left[M_{xy}^{(2)}+\frac{1}{2}h_2(N_{xy}^{(1)}-N_{xy}^{(3)})\right]\delta\varphi_2|_{y=0}^{b}=0$$
$$\left(M_{xy}^{(3)}-\frac{1}{2}h_3N_{xy}^{(3)}\right)\delta\varphi_3|_{y=0}^{b}=0$$
$$\left(M_{yy}^{(1)}+\frac{1}{2}h_1N_{yy}^{(1)}\right)\delta\gamma_1|_{y=0}^{b}=0$$
$$\left[M_{yy}^{(2)}+\frac{1}{2}h_2(N_{yy}^{(1)}-N_{yy}^{(3)})\right]\delta\gamma_2|_{y=0}^{b}=0$$
$$\left(M_{yy}^{(3)}-\frac{1}{2}h_3N_{yy}^{(3)}\right)\delta\gamma_3|_{y=0}^{b}=0 \tag{A14}$$

References

[1] Ross, D., Ungar, E. E., and Kerwin, E. M., "Damping of Plate Flexural Vibrations by Means of Viscoelastic Laminates," *Structural Damping*, ASME, New York, 1959, pp. 49–88.

[2] Sadasiva,Y., and Nakra, B. C., "Vibrations of Unsymmetrical Sandwich Beams and Plates with Viscoelastic Cores," *Journal of Sound and Vibration*, Vol. 34, No. 3, 1974, pp. 309–326. doi:10.1016/S0022-460X(74)80315-9

[3] Lu, Y. P., Killian, J. W., and Everstine, G. C., "Vibrations of 3 Layered Damped Sandwich Plate Composites," *Journal of Sound and Vibration*, Vol. 64, No. 1, 1979, pp. 63–71. doi:10.1016/0022-460X(79)90572-8

[4] Johnson, C. D., and Kienholz, D. A., "Finite-Element Prediction of Damping in Structures with Constrained Viscoelastic Layers," *AIAA Journal*, Vol. 20, No. 9, 1982, pp. 1284–1290. doi:10.2514/3.51190

[5] Lall, A. K., Asnani, N. T., and Nakra, B. C., "Vibration and Damping Analysis of Rectangular Plate with Partially Covered Constrained Viscoelastic Layer," *Journal of Vibration Acoustics Stress and Reliability in Design*, Vol. 109, No. 3, 1987, pp. 241–247.

[6] Cupial, P., and Niziol, J., "Vibration and Damping Analysis of a 3-Layered Composite Plate with a Viscoelastic Mid-Layer," *Journal of Sound and Vibration*, Vol. 183, No. 1, 1995, pp. 99–114. doi:10.1006/jsvi.1995.0241

[7] Kung, S. W., and Singh, R., "Complex Eigensolutions of Rectangular Plates with Damping Patches," *Journal of Sound and Vibration*, Vol. 216, No. 1, 1998, pp. 1–28. doi:10.1006/jsvi.1998.1644

[8] Gao, J. X., and Shen, Y. P., "Vibration and Damping Analysis of a Composite Plate with Active and Passive Damping Layer," *Applied Mathematics and Mechanics*, Vol. 20, No. 10, 1999, pp. 1075–1086.
doi:10.1007/BF02460324

[9] Wang, G., Veeramani, S., and Wereley, N. M., "Analysis of Sandwich Plates with Isotropic Face Plates and a Viscoelastic Core," *Journal of Vibration and Acoustics*, Vol. 122, No. 3, 2000, pp. 305–312.
doi:10.1115/1.1303065

[10] Jeung, Y. S., and Shen, I. Y., "Development of Isoparametric, Degenerate Constrained Layer Element for Plate and Shell Structures," *AIAA Journal*, Vol. 39, No. 10, 2001, pp. 1997–2005.
doi:10.2514/2.1192

[11] Yeh, J. Y., and Chen, L. W., "Vibration of a Sandwich Plate with a Constrained Layer and Electrorheological Fluid Core," *Composite Structures*, Vol. 65, No. 2, 2004, pp. 251–258.
doi:10.1016/j.compstruct.2003.11.004

[12] Hu, M. Y., and Wang, A. W., "Free Vibration and Transverse Stresses of Viscoelastic Laminated Plates," *Applied Mathematics and Mechanics*, Vol. 30, No. 1, 2009, pp. 101–108.
doi:10.1007/s10483-009-0111-y

[13] Arikoglu, A., and Ozkol, I., "Vibration Analysis of Composite Sandwich Beams with Viscoelastic Core by Using Differential Transform Method," *Composite Structures*, Vol. 92, No. 12, 2010, pp. 3031–3039.
doi:10.1016/j.compstruct.2010.05.022

[14] Le Maoût, N., Verron, E., and Bégué, J., "Simultaneous Geometrical and Material Optimal Design of Hybrid Elastomer/Composite Sandwich Plates," *Composite Structures*, Vol. 93, No. 3, 2011, pp. 1153–1157.
doi:10.1016/j.compstruct.2010.10.008

[15] Le Maoût, N., Verron, E., and Bégué, J., "On the Use of Discontinuous Elastomer Patches to Optimize the Damping Properties of Composite Sandwich Plates," *Composite Structures*, Vol. 93, No. 11, 2011, pp. 3057–3062.
doi:10.1016/j.compstruct.2011.04.023

[16] Golla, D. F., and Hughes, P. C., "Dynamics of Viscoelastic Structures: A Time-Domain, Finite-Element Formulation," *Journal of Applied Mechanics*, Vol. 52, No. 4, 1985, pp. 897–906.
doi:10.1115/1.3169166

[17] McTavish, D. J., and Hughes, P. C., "Modeling of Linear Viscoelastic Space Structures," *Journal of Vibration and Acoustics*, Vol. 115, No. 1, 1993, pp. 103–110.
doi:10.1115/1.2930302

[18] Lesieutre, G. A., and Bianchini, E., "Time Domain Modeling of Linear Viscoelasticity Using Anelastic Displacement Fields," *Journal of Vibration and Acoustics*, Vol. 117, No. 4, 1995, pp. 424–430.
doi:10.1115/1.2874474

[19] Galucio, A. C., Deu, J. F., and Ohayon, R., "Finite Element Formulation of Viscoelastic Sandwich Beams Using Fractional Derivative Operators," *Computational Mechanics*, Vol. 33, No. 4, 2004, pp. 282–291.
doi:10.1007/s00466-003-0529-x

[20] Pritz, T., "Five-Parameter Fractional Derivative Model for Polymeric Damping Materials," *Journal of Sound and Vibration*, Vol. 265, No. 5, 2003, pp. 935–952.
doi:10.1016/S0022-460X(02)01530-4

[21] Bellman, R., Casti, J., and Kashef, B. G., "Differential Quadrature: Technique for Rapid Solution of Nonlinear Partial Differential Equations," *Journal of Computational Physics*, Vol. 10, No. 1, 1972, pp. 40–52.
doi:10.1016/0021-9991(72)90089-7

[22] Shu, C., and Richards, B. E., "Application of Generalized Differential Quadrature to Solve 2-Dimensional Incompressible Navier–Stokes Equations," *International Journal for Numerical Methods in Fluids*, Vol. 15, No. 7, 1992, pp. 791–798.
doi:10.1002/fld.1650150704

[23] Moradi, S., and Taheri, F., "Differential Quadrature Approach for Delamination Buckling Analysis of Composites with Shear Deformation," *AIAA Journal*, Vol. 36, No. 10, 1998, pp. 1869–1873.
doi:10.2514/2.280

[24] Tornabene, F., and Viola, E., "2-D Solution for Free Vibrations of Parabolic Shells Using Generalized Differential Quadrature Method," *European Journal of Mechanics. A, Solids*, Vol. 27, No. 6, 2008, pp. 1001–1025.
doi:10.1016/j.euromechsol.2007.12.007

[25] Lin, R. M., Lim, M. K., and Du, H., "Deflection of Plates with Nonlinear Boundary Supports Using Generalized Differential Quadrature," *Computers and Structures*, Vol. 53, No. 4, 1994, pp. 993–999.
doi:10.1016/0045-7949(94)90385-9

[26] Tornabene, F., and Viola, E., "Vibration Analysis of Spherical Structural Elements Using the GDQ Method," *Computers and Mathematics with Applications*, Vol. 53, No. 10, 2007, pp. 1538–1560.
doi:10.1016/j.camwa.2006.03.039

[27] Jones, D. I. G., *Handbook of Viscoelastic Vibration Damping*, Wiley, New York, 2001, pp. 180, 184.

[28] Drake, M. L., "Damping Properties of Various Materials," AFWAL TR-88-4248, 1988.

[29] Araujo, A. L., Soares, C. M. M., Soares, C. A. M., and Herskovits, J., "Optimal Design and Parameter Estimation of Frequency Dependent Viscoelastic Laminated Sandwich Composite Plates," *Composite Structures*, Vol. 92, No. 9, 2010, pp. 2321–2327.
doi:10.1016/j.compstruct.2009.07.006

[30] Araujo, A. L., Soares, C. M. M., Soares, C. A. M., and Herskovits, J., "Characterisation by Inverse Techniques of Elastic, Viscoelastic and Piezoelectric Properties of Anisotropic Sandwich Adaptive Structures," *Applied Composite Materials*, Vol. 17, No. 5, 2010, pp. 543–556.
doi:10.1007/s10443-010-9142-2

[31] de Lima, A. M. G., Stoppa, M. H., Rade, D. A., and Steffen, V., "Sensitivity Analysis of Viscoelastic Structures," *Shock and Vibration*, Vol. 13, Nos. 4–5, 2006, pp. 545–558.

[32] Mantena, P. R., Gibson, R. F., and Hwang, S. J., "Optimal Constrained Viscoelastic Tape Lengths for Maximizing Damping in Laminated Composites," *AIAA Journal*, Vol. 29, No. 10, 1991, pp. 1678–1685.
doi:10.2514/3.10790

[33] Tanimoto, T., "Carbon-Fiber Reinforced Plastic Passive Composite Damper by Use of Piezoelectric Polymer/Ceramic," *Japanese Journal of Applied Physics*, Part 1, Vol. 41, No. 11B, 2002, pp. 7166–7169.
doi:10.1143/JJAP.41.7166

N. Wereley
Associate Editor